



Grid Integration of Multistring Photovoltaic Plants with Modular Multilevel Converter

Ahmad Kamal, Dr. Abdul Basit

Abstract—This paper presents the application of Modular Multilevel Converter (MMC) for connecting multistring photovoltaic generation plant. The proposed approach makes it possible for an increased PV plant capacity to be integrated with the grid, while also improving efficiency of conversion and power quality. To increase the efficiency of individual PV module, a DC-DC boost converter is employed with maximum power point tracking (MPPT). The MPPT is implemented by employing Perturb & Observe (P&O) algorithm. The PV modules with DC-DC boost converters are connected in parallel to form a DC bus which is connected to the utility grid with MMC. The MMC inverts the DC bus voltage for interfacing to the grid while maintaining the DC bus voltage constant. The simulation of the overall system in Simulink/MATLAB verifies the validity of the proposed system.

Keywords— Renewable integration, Modular Multilevel Converter, maximum power point tracking, MPPT, photovoltaic system

I. INTRODUCTION

The continuously growing demand for energy and depletion of fossil fuels has increased the need for efficient integration of renewable resources in the current grid [1]. Solar PV energy has seen a tremendous increase over the past few years. The steady reduction in manufacturing cost of PV modules is the contributing factor towards this growth. This growth is evident from the fact that in 2013 alone, 30 GW of new PV capacity was installed. It is encouraging that the PV integration has increased to more than 100 GW since 2012 [2].

There are basically two main topologies to connect large scale PV systems to the grid: the multistring configuration and the centralized configuration [3, 4]. In the centralized configuration several PV strings are connected in parallel to dc bus. A voltage source converter is used to invert the DC voltage to the grid while also implementing MPPT for all the connected PV strings. The multistring configuration has a similar structure with the centralized configuration with the exception that the PV strings are connected to the DC bus with individual DC-DC boost converters.

The individual DC-DC boost converter perform MPPT for

each PV string exclusively and thus can produce more power than the centralized configuration. The voltage source converter in the centralized configuration also has to tackle the issues of partial shading and panel mismatch increasing its complexity. Owing to these facts the multistring configuration is preferred over the centralized configuration even with the increased initial cost of the DC-DC boost converters.

The increase in PV farms of MW capacity require a significant increase in the power handling capability of the grid tied converter. The traditional voltage source converters with two level topology is incapable of efficiently handling this higher power flow. Also the grid codes applied on such PV farms continue to demand efficient integration [5]. The multilevel converters offer several benefits over the traditional two-level topology such as higher power and voltage ratings, lower switching frequency and total harmonic distortion (THD) [6]. Due to these advantages, multilevel converters are gaining popularity in many applications such as motor drives, traction and even in renewable integration [7].

Most of the literature on using multilevel converters for grid interface of PV farms proposes the use of neutral point clamped (NPC) and cascaded H bridge (CHB) based multilevel converters. The studies of [8] and [9] propose a three level neutral point clamped (3L-NPC) multilevel converter with two PV strings. The PV strings are connected without a DC-DC converter with the two DC-link capacitors, enabling MPPT capability for each string. However, the lack of DC-DC boost converter requires several panels to be connected in series for raising the string voltage to be NPC compatible. This series connection of panels introduces the problems of efficient MPPT implementation, partial shading and panel mismatch. Additionally, as the DC-link capacitors have to operate at different MPPT voltages this can cause dc-link unbalance and thus introducing distortions at the grid side. This imbalance of DC-link may also have negative impacts on AC side control of the converter.

The studies of [10] and [11] propose Cascaded H-bridge (CHB) multilevel converters for this application. The CHB topology is implemented on a single phase system, due to the intrinsic power unbalance of each phase. This is not allowed by the grid codes due to the injection of unbalance currents into the grid. Additionally, this topology also has the disadvantages associated with the NPC multilevel converters discussed above.

This paper presents multistring PV system with three phase modular multilevel converter (MMC). Each PV string is

Ahmad Kamal: Department of Electrical Energy Systems Engineering US-PCAS-E, UET Peshawar, Paksitan. (e-mail: engr.ahmad.kamal@live.com)

Dr. Abdul Basit: Department of Electrical Energy Systems Engineering US-PCAS-E, UET Peshawar, Paksitan. (e-mail: abdul.basit@uetpeshawar.edu)

connected to a common DC bus with individual DC-DC boost converters with MPPT capability. The remainder of the paper is divided into four sections. Section II depicts the overall system structure and describes all the three stages that the overall system is divided into. Section III explains the overall control system which is further subdivided into 4 subsections that is: boost stage control, MMC output current control, MMC circulating current control and MMC submodule voltage balance control. The system parameters, simulation and the results are presented in section IV. Finally, the conclusion of the study is presented in section V.

II. OVERALL SYSTEM DESCRIPTION

The detailed circuit of the proposed overall system is illustrated in Figure 1. The system has basically three major stages: PV string stage, DC-DC boost converter stage and the grid-tied three phase modular multilevel converter (MMC). It should be noted that only a single phase of the MMC converter is displayed in this illustration. The PV strings are formed by connecting several PV modules in series to raise the voltage level to the desired level. For connecting the PV string to DC bus any topology of the DC-DC boost converter can be used according to specific requirements. In this study, the typical boost converter topology is used due to simplicity and ease of simulation.

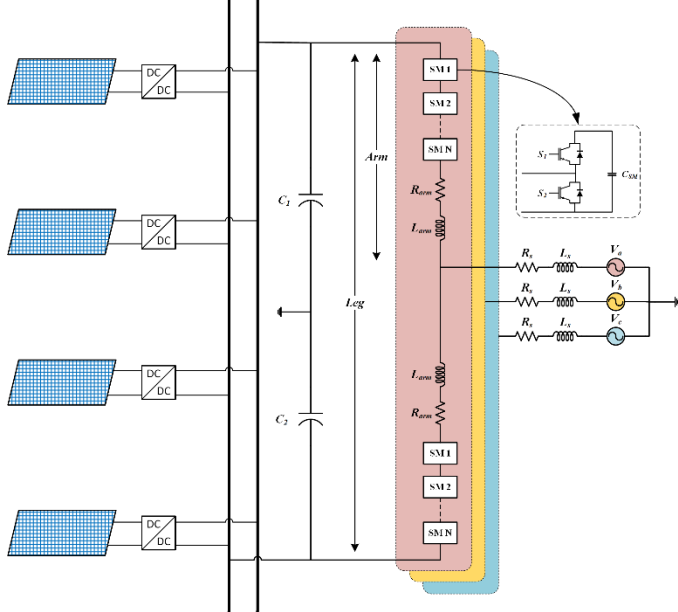


Figure 1. Proposed system configuration

Modular multilevel converter is a relatively newer topology of multilevel converters for medium to high voltage applications. Modular multilevel converter has many advantages compared with the traditional multilevel converters such as: minimizing the total harmonic distortion (THD) on output voltage, operating with lower switching frequency, low dv/dt thus lower stresses on power switches and operating with any voltage level.

The basic building block of the MMC is a submodule. It is essentially a half bridge inverter with capacitor as shown in

Figure 1. The half bridge can be constituted with any power switch such as IGBT, IGCT or MOSFET with antiparallel diode, according to specific requirements. The two switches of the submodule operate in a complimentary fashion. When switch S_2 of the submodule is turned-on the submodule capacitor voltage becomes the output voltage of the submodule. When S_1 is turned-on the submodule is essentially turned-off, or in the case of MMC referred to as being bypassed. When N number of submodules are connected in series it forms an ‘arm’ of the MMC as shown in Figure 1. Two arms combine together to form the individual phase, called the ‘leg’ of the MMC.

The number of output voltage levels generated by the MMC can be with either $N+1$ or $2N+1$ depending on the modulation strategy used. The three main modulation strategies used for MMC are the pulse width modulation (PWM), space vector modulation and the nearest level modulation. The modulation strategy used in this study is the carrier phase shifted PWM.

The benefit of using the modular multilevel converter is the modularity of the system which means that the system can be scaled from small KW level to large MW level PV systems.

III. CONTROL SYSTEM

Decoupling MPPT control from the grid converter makes it possible to design and implement control for DC-DC boost converter and MMC independently.

A. DC-DC Boost Converter Control

The main control objective of the DC-DC boost converter is to implement the MPPT algorithm for the PV string while stepping up the string voltage.

The controllable variable of the DC-DC boost converter is the inductor current. This inductor current can control either the input voltage or the output voltage of the DC-DC boost converter. As the output voltage of the converter, that is the DC bus voltage, is controlled by the grid-tied MMC so the boost converter controls the input voltage. The input voltage of the DC-DC boost converter in continuous conduction mode is given by the following equation.

$$V_{in} = V_{out} (1 - D) \quad (1)$$

As V_{out} is controlled by the MMC, changing the duty cycle D of the converter changes the input voltage V_{in} , which is essentially the PV string voltage. Figure 2 shows the control structure of the DC-DC boost converter.

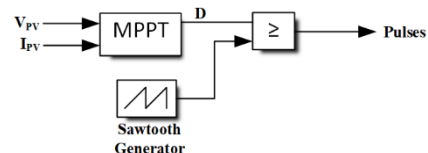


Figure 2. Boost converter control with MPPT

The MPPT algorithm used in this study is the well-known Perturb and Observe (P&O) algorithm. The output of the control structure ‘Pulses’ are the pulses that drive the power switch of the boost converter. The flowchart for the Perturb and Observe (P&O) MPPT algorithm is depicted in Figure 3.

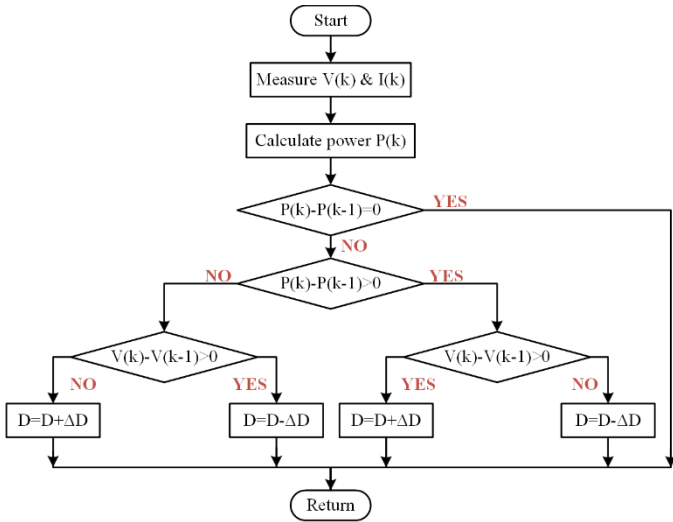


Figure 3. Perturb and Observe (P&O) MPPT flowchart

B. MMC Output Current Control

The control scheme for output current control of MMC is similar to that of two level converters control in dq rotating reference frame [12]. The control system is divided into two control loops: inner control loop and outer control loop. The outer control loop controls the DC bus voltage by generating reference signal for d-axis current. The relationship between DC bus voltage V_{dc} and d-axis current i_d can be derived from AC side and DC side power balance of MMC, given as:

$$P = \frac{3}{2} V_d i_d = V_{dc} i_{dc} \quad (2)$$

$$i_{dc} = C \frac{dV_{dc}}{dt} \quad (3)$$

Transferring to s domain and combining (2) and (3) the system transfer function is given as:

$$\frac{V_{dc}(s)}{i_d(s)} = \frac{3V_d}{2V_{dc,ref}} \cdot \frac{1}{sC} \quad (4)$$

The above system transfer function is used to derive the control system for DC voltage control, shown in Figure 4.

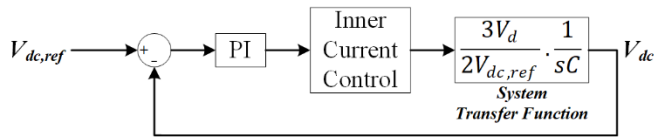


Figure 4. DC voltage control loop

The inner control structure can be deduced from the dynamic equations of the MMC, given as:

$$L_s \frac{di_j}{dt} = -R_s i_j + V_g - V_t \quad (5)$$

The above dynamic equation in the dq-frame is given as:

$$L_s \frac{di_d}{dt} = -R_s i_d + V_{gd} - V_{td} + \omega L i_q \quad (6a)$$

$$L_s \frac{di_q}{dt} = -R_s i_q + V_{gq} - V_{td} - \omega L i_d \quad (6b)$$

In the above equations, V_{td} , V_{tq} , i_d , i_q , V_{gd} , V_{gq} , $\omega L i_d$, $\omega L i_q$ are d and q axis components of MMC output voltage,

output current, grid voltage and coupling terms respectively. Based on the above equations, the architecture of the inner current control loop is derived as in Figure 5.

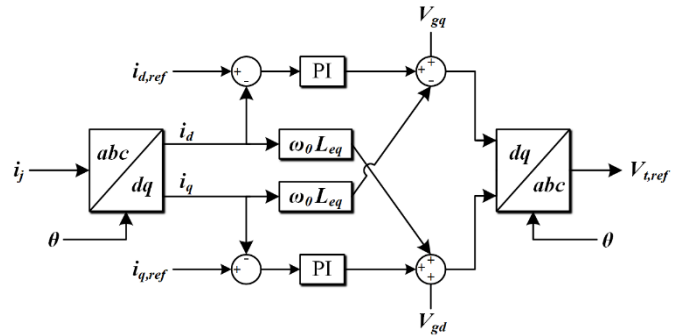


Figure 5. Inner current control loop

C. MMC Circulating Current Control

The floating nature of the submodule capacitors results in a circulating current that flows from the DC bus to the MMC and between different phases of MMC. The harmonic components of the circulating current does not contribute in power transfer but increases power losses and current rating of electrical components. Therefore, the major component of the harmonic components, the second harmonic component, is controlled to zero. This circulating current can be represented by the following equation:

$$i_{cc,j} = \frac{i_{uj} + i_{lj}}{2} - \frac{I_{dc}}{3} \quad (7)$$

Substituting the above equation in dq-frame in the dynamic equations of the MMC gives the following relationship:

$$V_{cc,d} = R_{arm} i_{cc,d} + L_{arm} \frac{di_{cc,d}}{dt} + 2L_{arm} \omega i_{cc,q} \quad (8a)$$

$$V_{cc,q} = R_{arm} i_{cc,q} + L_{arm} \frac{di_{cc,q}}{dt} - 2L_{arm} \omega i_{cc,d} \quad (8b)$$

Considering the above equations, it is evident that the circulating current can be controlled directly by $V_{cc,d}$ and $V_{cc,q}$ as shown in Figure 6. The output of this circulating current controller will be subtracted from both lower and upper arm voltage references generated by inner current loop.

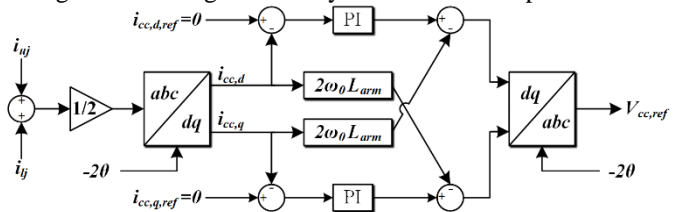


Figure 6. Circulating current control loop

D. MMC Submodule Voltage Balancing Control

The floating nature of the submodule capacitors has the adverse impact that the capacitor voltages diverge with time. This divergence if not kept small or preferably negligible can collapse the entire system. Therefore, to keep the submodule voltages equal an active balancing algorithm is required.

The most widely used method for this purpose is the sorting method [13]. Generally, the number of submodules to be inserted in each arm is known after modulation. The decision

of which submodules to insert or bypass, to balance the submodule voltages, is taken by the sorting algorithm. The algorithm first measures and sorts all the submodules capacitor voltages. Submodules with the lowest voltages are inserted to be charged if the arm current is positive. Whereas, submodules with the highest voltages are inserted to be discharged if the arm current is negative. However, bypassing the submodule keeps its voltage unchanged.

IV. SIMULATION & RESULTS

The whole system with the control schemes was simulated in Simulink/MATLAB. Since the simulation used detail models of all the converters, and the system was simulated with different temperature and irradiation levels, only four PV string with individual boost converters were used. The panels used in the simulation were SunPower SPR-315E-WHT-D rated at 315W, with output current of 5.76A and 54.7V output voltage at MPP at STC (radiation of 1000W/m^2 and panel temperature of 25°C). A single PV array is built with 64 modules in series per string and 5 strings in parallel. The DC-DC boost converter stage steps up the voltage of the PV array to 500V of the DC bus voltage. As the DC bus voltage is 500V the number of submodules per arm are selected to be 6. This is considering the voltage rating of the submodule is to be kept at 100V, which makes it possible to use a wide variety of power switches. The system parameters used for the simulation are summarized in Table 1.

TABLE I
OVERALL SYSTEM PARAMETERS

Symbol	Quantity	Value
V_g	Grid voltage	11KV
f	Grid frequency	60Hz
L_s	Grid inductance	45 μF
R_s	Grid resistance	1m Ω
L_{arm}	MMC arm inductance	60 μH
R_{arm}	MMC arm resistance	1m Ω
C_{SM}	MMC submodule capacitance	96mF
V_{dc}	DC-link voltage	500V
C_1, C_2	DC-link voltage capacitance	1mF
L_b	Boost converter inductance	5mH
V_{mp}	PV array voltage at maximum power	274.5V
I_{mp}	PV array current at maximum power	367.2A
T_s	Sampling Time	50 μs

The MPPT performance is evaluated with different levels of irradiance and ambient temperature as shown in Figure 7. The resulting varying duty ratio, array voltage and power is depicted in the same figure. To validate the performance of the DC bus voltage control of the MMC, the irradiance level of all the converters connected with the DC bus are varied as shown in Figure 8. It can be seen that the varying irradiance level changes the combined power output of all the PV modules but the DC bus voltage stays relatively unchanged.

The performance of the circulating current suppression control of the MMC can be evaluated from Figure 9, which shows the circulating current, upper arm current and submodule capacitor voltages of phase A. The circulating current suppression control is enabled at $T=0.2\text{s}$, resulting in a

significant decrease in the circulating current, arm current and submodule capacitor peak-peak voltage.

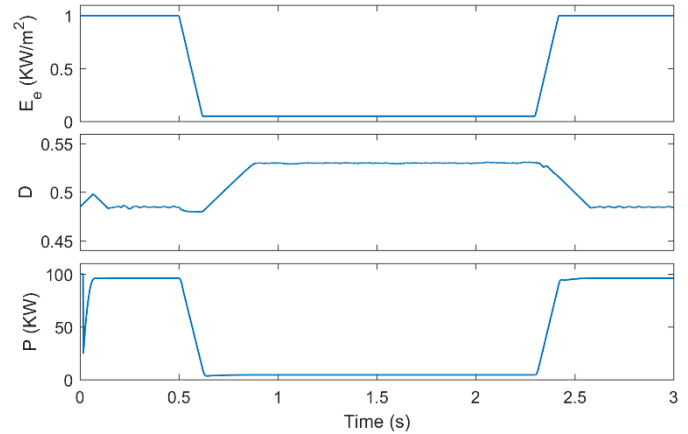


Figure 7. PV array 1 irradiance, duty cycle and power

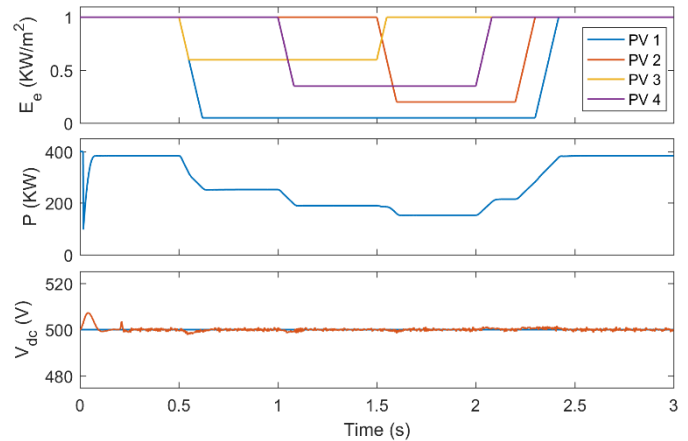


Figure 8. PV farm output power and dc bus voltage with varying irradiance

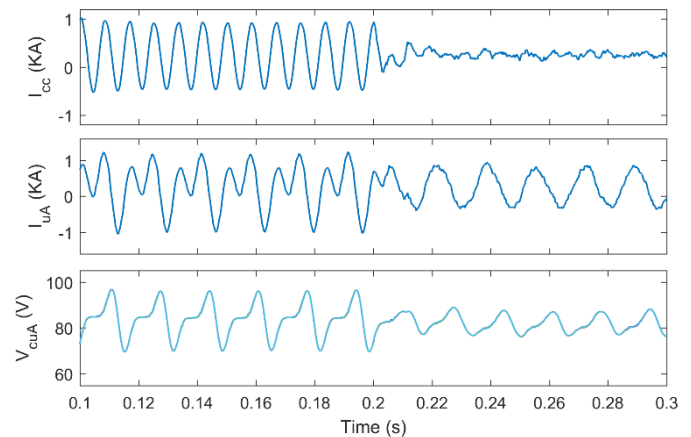


Figure 9. Performance of circulating current control

The effectiveness of the voltage balancing algorithm can be validated from Figure 10, which compares the submodule capacitor voltages of phase A upper arm with and without voltage balancing algorithm.

Finally, the steady state three phase output voltages and currents of the MMC are displayed in Figure 11. The steady

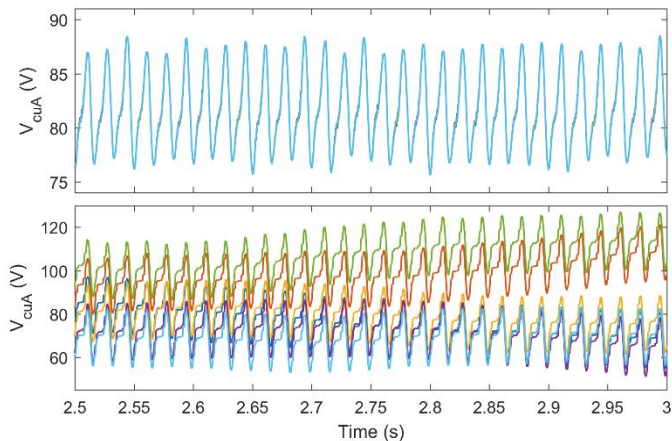


Figure 10. Performance of voltage balancing algorithm

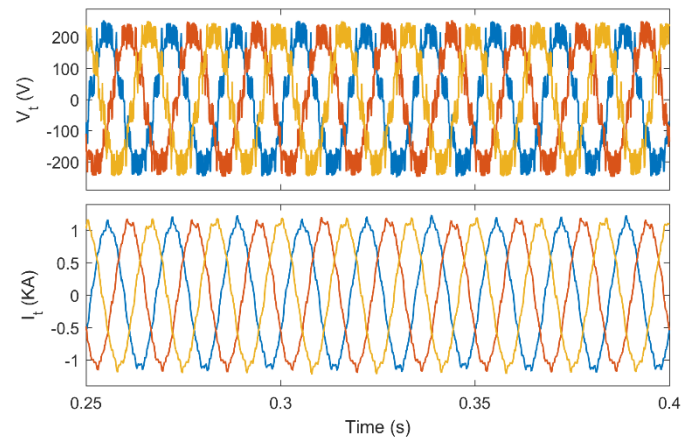


Figure 11. Steady-state output voltage and current of MMC

state output shows a satisfactory performance with a 4.5% total harmonic distortion of currents.

V. CONCLUSION

The proposed multistring photovoltaic DC bus energy conversion system with modular multilevel converter is capable of interfacing a large MW scale PV farm with the grid. Individual DC-DC boost converters for PV arrays increase system efficiency by better implementation of MPPT algorithm. The use of modular multilevel converter improves power quality, overall efficiency and reduces switching frequency compared to the traditional 2L-VSC. The modular multilevel converter also makes it possible to easily scale the system to any power level.

REFERENCES

- [1] A. M. T. O. A. S. A. P. W. a. M. A. G. Shafiullah, "Meeting energy demand and global warming by integrating renewable energy into the grid," in *2012 22nd Australasian Universities Power Engineering Conference (AUPEC)*, Bali, 2012.
- [2] European Photovoltaic Industry Association, "Global market outlook for photovoltaics 2013–2017," 2013.
- [3] J. K. P. a. F. B. S. B. Kjaer, "A review of single-phase grid-connected inverters for photovoltaic modules," *IEEE Transactions on Industry Applications*, vol. 41, no. 5, pp. 1292-1306, Oct. 2005.
- [4] M. M. a. G. Cramer, "Multi-String-Converter: The next step in Evolution of String-Converter Technology," in *9th European Conference on Power Electronics and Applications*, Graz, Austria, Aug. 2001.
- [5] E. B.-M. M. A.-P. O. G.-B. Ana Cabrera-Tobar, "Review of advanced grid requirements for the integration of large scale photovoltaic power plants in the transmission system," *Renewable and Sustainable Energy Reviews*, vol. 62, pp. 971-987, Sep 2016.
- [6] J.-S. L. a. F. Z. P. J. Rodriguez, "Multilevel inverters: a survey of topologies, controls, and applications," *IEEE Transactions on Industrial Electronics*, vol. 49, no. 4, pp. 724-738, Aug. 2002.
- [7] M. C. a. V. G. Agelidis, "Multilevel converters for single-phase grid connected photovoltaic systems-an overview," in *Industrial Electronics, 1998. Proceedings. ISIE '98. IEEE International Symposium*, Jul. 1998.
- [8] M. L. R. T. C. K. a. M. S. T. Kerekes, "Evaluation of Three-phase Transformerless Photovoltaic Inverter Topologies," *IEEE Trans. Power Electronics*, vol. 24, no. 9, pp. 2202-2211, Sep. 2009.
- [9] S. O. a. L. M. T. E. Ozdemir, "Fundamental-frequency-modulated Six-level Diode-clamped Multilevel Inverter for Three-phase Stand-alone Photovoltaic System," *IEEE Trans. Industrial Electronics*, vol. 56, no. 11, pp. 4407-4415, Nov. 2009.
- [10] P. C. J. R. a. M. P. E. Villanueva, "Control of a Single-phase Cascaded H-bridge Multilevel Inverter for Grid-connected Photovoltaic Systems," *IEEE Trans. Industrial Electronics*, vol. 56, no. 11, pp. 4399-4406, Nov. 2009.
- [11] A. M. E. V. P. C. B. W. a. J. R. S. Kouro, "Control of a cascaded h-bridge multilevel converter for grid connection of photovoltaic systems," in *35th Annual Conference of the IEEE Industrial Electronics Society (IECON09)*, Porto, Portugal, Nov. 2009.
- [12] S. B. J. R. S. K. a. R. L. M. A. Perez, "Circuit Topologies, Modeling, Control Schemes, and Applications of Modular Multilevel Converters," *IEEE Transactions on Power Electronics*, vol. 30, no. 1, pp. 4-17, Jan. 2015.
- [13] J. Q. B. B. M. S. a. P. B. S. Debnath, "Operation, Control, and Applications of the Modular Multilevel Converter: A Review," *IEEE Transactions on Power Electronics*, vol. 30, no. 1, pp. 37-53, Jan. 2015.